SAND2022-0722J

https://doi.org/10.1016/j.fuel.2021.122569

# Machine-learning based prediction of injection rate and solenoid voltage characteristics in GDI injectors

Heechang Oh[a*], Joonsik Hwang[b], Lyle M. Pickett[c] ,Donghee Han[a]

[a] R&D division, Hyundai Motor Company, Hwaseoung-si,Gyeonggi-do, 18290, Republic of Korea

[b] Department of Mechanical Engineering, Mississippi State University, Mississippi State, MS 39762, USA

[c] Combustion Research Facility, Sandia National Laboratories, Livermore, CA 94550, USA

**Abstract**

Current state-of-the-art gasoline direct-injection (GDI) engines use multiple injections as one of the key technologies to improve exhaust emissions and fuel efficiency. For this technology to be successful, secured adequate control of fuel quantity for each injection is mandatory. However, nonlinearity and variations in the injection quantity can deteriorate the accuracy of fuel control, especially with small fuel injections. Therefore, it is necessary to understand the complex injection behavior and to develop a predictive model to be utilized in the development process. This study presents a methodology for rate of injection (ROI) and solenoid voltage modeling using artificial neural networks (ANNs) constructed from a set of Zeuch-style hydraulic experimental measurements conducted over a wide range of conditions. A quantitative comparison between the ANN model and the experimental data shows that the model is capable of predicting not only general features of the ROI trend, but also transient and non-linear behaviors at particular conditions. In addition, the end of injection (EOI) could be detected precisely with a virtually generated solenoid voltage signal and the signal processing method, which applies to an actual engine control unit. A correlation between the detected EOI timings calculated from the modeled signal and the measurement results showed a high coefficient of determination.

**Keywords**: Machine-learning; Artificial Neural Network (ANN); Gasoline Direct Injection (GDI); Rate of Injection; Injection, Gasoline engine

[*]Contact information: Heechang Oh, Senior Researcher at Hyundai Motor Company.

Tel.:+82-10-7425-5009, e-mail: disi@hyundai.com

https://doi.org/10.1016/j.fuel.2021.122569

**Abbreviations**

| | | | |
|---|---|---|---|
| ANN | Artificial neural network | ICE | Internal combustion engine |
| CFD | Computational fluid dynamics | ICLC | Injector closed-loop control |
| COSI | Controlled Solenoid Injection | ML | Machine-learning |
| ECU | Engine control unit | NVH | Noise, vibration, and harshness |
| EMF | Electromotive force | PFI | Port fuel injection |
| EOI | End of injection | ROI | Rate of injection |
| GDI | Gasoline direct-injection | SOI | Start of injection |
| HDA | Hydraulischen Druckanstieg Analysator | VCI | Valve Controlled Injection |

**Nomenclature**

| | | | |
|---|---|---|---|
| $a$ | Speed of sound [m/s] | $\rho$ | Density of the fuel [kg/m$^3$] |
| ΔP | Pressure difference across the nozzle | $t_{boost}$ | Solenoid boosting phase [ms] |
| m | Injected mass [kg] | $t_{close}$ | Valve closing delay [ms] |
| $t_{EOI}$ | End of injection timing [ms] | $t_{hold}$ | Solenoid holding phase [ms] |
| $t_{inj}$ | Coil energizing time [ms] (injection command pulse duration) | $t_{peak}$ | Solenoid picking phase [ms] |
| $t_{open}$ | Valve opening delay [ms] | $t_{SOI}$ | Start of injection timing [ms] |
| m | Injected mass [kg] | $T_{fuel}$ | Fuel temperature [°C] |
| $Q_{\mathrm{stat}}$ | Static flow rate [g/min] | $\mathrm{q_{i,j}}$ | Regression weight vector at (i,j) [a.u.] |
| V | fixed volume of the chamber [m3] | $\mathrm{x_k}$ | Feature vector for training [a.u.] |
| $R^2$ | Coefficient of determination | | |

## 1. Introduction

Automobile manufacturers are trying to reduce the $CO_2$ emissions from vehicles to meet the tightening emission regulations all over the world. As such, manufacturers are increasing the volume of zero tailpipe emission vehicles such as battery-electric and fuel cell electric vehicles [1][2]. In addition, hybrid electric vehicles which have both an

https://doi.org/10.1016/j.fuel.2021.122569

internal combustion engine (ICE) and an electric propulsion system, are also regarded to be the important solution for the cleaner powertrain technology and they are expected to have larger market shares in the near future [3][4]. Since hybrid electric vehicles still have ICEs, the improvement of thermal efficiency and emissions from ICEs is essential to achieve further reduction of $CO_2$ emissions in the transportation sector [5]. Numerous research activities are focused on the optimization of the combustion system and control strategies of ICEs in different aspects.

One of the most important technologies in modern gasoline engines is gasoline direct injection (GDI). Different from the previous fuel delivery method called port fuel injection (PFI), the GDI engines inject fuel directly into the combustion chamber. GDI engines have the advantages in reducing knocking combustion thanks to evaporation cooling and enhancement of in-cylinder flow and turbulence through fuel injection [6][7]. In particular, in the case of the latter effect, great progress has been carried out on the catalyst light-off time reduction under cold-start conditions with the GDI technology. Current state-of-the-art GDI engines utilize multiple injections up to 5 times under cold start catalyst heating conditions to minimize undesired spray impingement and to ensure combustion stability under the aggressively retarded combustion phasing condition by supplying injection-driven flow and turbulence [8][9]. This enables the reduction of exhaust emissions during the catalyst heating operation as well as faster catalyst activation with minimized vehicle noise, vibration, and harshness (NVH). Optimizations in injector nozzle, spray geometry, and injection strategy are crucial in this aspect. However, precise control in injection quantity is of utmost importance in advance. To take advantage of the multiple injection strategies, the repeatability and consistency of the injection quantity control must be secured. Otherwise, it would fail to control combustion stability and air-fuel ratio. Therefore, it is necessary to minimize the variation in the injection quantity for different injection events, different engine conditions, and different injectors.

Injection quantity is known to be proportional to the duration of the coil energizing time (electrical command duration) applied to the GDI injector. However, for a case using a very small injection quantity such as pilot injections, the correlation between coil energizing time and injected fuel amount becomes highly nonlinear and accompanies sample-to-sample variation as shown in Fig. 1. The nonlinear behavior, which also is related with shot-to-shot variation, are mainly caused by the transient behavior of the needle and the armature during valve opening and closing delays. In the same manner, sample-to-sample variations can occur under the small injection quantity conditions due to the tolerances of the mechanical and the electrical elements of each injector [10][11][12]. To mitigate sample-to-sample

https://doi.org/10.1016/j.fuel.2021.122569

variations and to enhance the repeatability of small injection quantities, the injection quantity diagnostics and compensation control strategy with solenoid signal feedback has been introduced in the 2010s [13][14]. Many different suppliers are using such technology denoted as controlled valve operation (CVO) for Bosch [13], injector closed-loop control (ICLC) for Delphi [14], Controlled Solenoid Injection (COSI) for Vitesco, and Valve Controlled Injection (VCI) for Hyundai Kefico. The common principle is to measure the actual valve opening and closing delays from the solenoid signal and correct the length of injection command pulse to be the actual valve opening period for the target injection quantity. This enables the utilization of GDI injectors with the smallest tolerances as well as the minimized shot-to-shot variation under various engine operating conditions. This measurement and correction can be performed on each injector and cylinder and thus, sample-to-sample and cylinder-to-cylinder variations can be minimized as well. These techniques commonly use the solenoid voltage signal to measure valve closing time to perform the correction of injection command pulse. When the coil energizing pulse ends, the solenoid driving current supplied from the driver falls to zero. As a result, the needle moves toward the valve seat by the spring force while the voltage of the solenoid also increased from the negative value. During this stage, solenoid voltage signal shows a transient response resulting from a combination of back-electromotive force (EMF) induced by armature movement and a natural response of the electrical circuit. Once the needle and armature are seated to default position, the EMF becomes zero, and only the natural response component remains. Therefore, there is an inflection point of the solenoid voltage curve at the actual valve closing timing and the time difference between this timing and the end of energizing time can be identified as valve closing delay. An example showing the injection current and corresponding rate of injection (ROI) and solenoid voltage signal are presented in Fig. 2. These detection and compensation techniques have been expanded to estimating the valve opening delay as well. These injection quantity control technology is regarded as the breakthrough technology to meet the stringent exhaust emission regulations and its technical importance is expected to increase even more in the future.

On the other hand, many automotive manufacturers are recently utilizing various simulation and modeling approaches to reduce the time and cost of the powertrain and vehicle development. These activities are increasingly being integrated into a ‘powertrain virtual development’ process and include a variety of tasks such as functional development of the component, system integration, and preliminary calibration processes beyond the traditional simulations [15][16][17]. For these developments, it is essential to develop and integrate accurate and efficient models. Among the required models, the fuel injection rate is one of the most important pieces of information needed for

engine modeling. Several methodologies have already been implemented for gasoline and diesel injection rate modeling.

One approach is computational fluid dynamics (CFD) simulation for the characterization of the internal-nozzle multi-phase flow [18][19]. This is a physics-based approach, so it can provide useful information not only on the injection rate, but also on also other important spray characteristics. However, it requires high computation cost. Another approach is one-dimensional hydraulic modeling of the injector, which has been most widely employed for the rate of injection (ROI) simulations due to the good trade-off between accuracy and computation cost [20][21][22][23]. However, the 1D modeling is based on the characterization of all components of the fuel injection system, requiring detailed understanding of all geometries and physical phenomena in the elements. Finally, there are zero-dimensional injector model approaches that employ empirical or mathematical expressions and correlations fitted to experimental data to produce reliable ROI estimation [24][25]. The accuracy of the simplified model can be improved through validation with the experimental results. The disadvantage of this approach is the high dependency on experimental data. Each of these approaches has its pros and cons, while it will be possible to select and use proper methodology by considering the purpose and available resources. However, if the development and verification of the injection control strategy such as the previously described feedback control algorithm is required in the virtual development process, none of the approaches described previously can help since these models cannot replicate the electromagnetic behavior of the injector. To predict the electromagnetic behavior of the injector correctly, the electromagnetic model should be implemented and coupled with existing ROI models, but this will greatly increase the complexity and the difficulty of the modeling.

On the contrary to the model-based approaches described above, there is a recent trend to apply artificial neural network (ANN) and machine-learning (ML) algorithms in the fuel spray research area [26][27][28][29]. Advances in experimental and data analysis are constantly accelerating the massive production of data across all fields. The analysis of those data through ANN and ML is offering novel breakthroughs in a wide variety of disciplines. As previously discussed, the physical or mathematical modeling for the prediction of ROI and solenoid electrical signals will be challenging tasks and it will require the complex modeling of coupled behavior of electromagnetic, hydraulic, and mechanical components. However, predictive models can be developed without physical modeling for complex systems through ML instead. Moreover, the ROI and the solenoid voltage signal have a small number of input

https://doi.org/10.1016/j.fuel.2021.122569

variables that can be simply expressed with numerical values and have the characteristic of a surjective function of which outputs have the form of a simple 1D curve. Therefore, they are believed that the difficulty of inductive regression modeling through ML is not high.

The primary objective is to establish a framework to predict ROI and solenoid voltage signal using a ML algorithm. We develop an ANN network for time-resolved ROI and voltage signals without any time-marching simulations. For the training, experimental data of various injectors having different Qstat under various injection conditions such as coil energizing time, fuel temperature, and the pressure difference across the nozzle were utilized. Inputs were composed of 4 parameters including Qstat and injection conditions. Based on the measurement results, independent models for ROI and solenoid voltage were separately developed and validated. To the best of the authors' knowledge, this is the first study in the literature to introduce a ML based methodology suitable for predicting and quantifying the injection rate and solenoid voltage signal of a state-of-the-art GDI injector under various operating conditions. In addition, the value of this study is to propose a useful methodology for fuel injection modeling that can be applied to the virtual powertrain development process. Since the model proposed in this study can predict not only the ROI but also the feedback signal required for the precise injection quantity control, The developed model can be used as a sub-model for the development, verification, and calibration of GDI injection control logic virtually and this will greatly reduce development time and cost.

## 2. Experimental set up and condition

### 2.1. Test injectors and fuel

Five GDI injectors having different Qstat were tested for the ROI and solenoid voltage signal measurement. Tested injectors are the state-of-the-art injector available in the market of which the maximum injection pressure is 350 bar. Specification for the test injectors are summarized in Table 1. The static flow rate shown in Table 1 is defined as the steady-state mass flow rate of the injector when n-heptane is injected with 100 bar of injection pressure under room temperature and atmospheric pressure conditions. All injectors share identical geometry for components such as valve seat, needle, armature, internal flow channel, and electromagnetic coil except for the number and size of nozzle holes to achieve different Qstat varying from 250 to 415 g/min.

https://doi.org/10.1016/j.fuel.2021.122569

To perform the test under the realistic conditions mimicking the gasoline engine, multi-component surrogate fuel for United State market fuel (E10 gasoline) was used instead of single component fuel, not representative of real gasoline, widely used in the ROI measurement. The surrogate fuel was developed under the Department of Energy's 'Partnership for Advanced Combustion Engines (PACE), A light-duty national laboratory combustion consortium' project. Detailed components and properties of the fuel are listed in Table 2.

**2.2. Experimental set up and conditions**

A schematic diagram of the injection rate measurement is shown in Fig. 3. The measurement system is composed of the test injector, high-pressure pump, the injection rate meter, and a function generator that sends command to the injector driver and injection rate meter synchronously. The injection pressure was controlled using a high-pressure syringe pump (Teledyne 30D). Genotec's universal injector driver (Solenoid Injector Power Amplifier V2) was used to generate the solenoid driving current profile supplied by the manufacturer. The solenoid voltage and current were measured from analog outputs of the injector driver. The Moehwald HDA (hydraulischen druckanstieg analysator) which is a commercially available injection rate measurement device was used in this study. Details of HDA and its measurement principle are well described in an earlier study [30]. HDA uses Zeuch's method that measures the change in hydraulic pressure that results from injecting fuel into a fuel-filled constant volume chamber while the sound speed of the fuel is also measured by the equipped ultrasonic sensor. The injection mass flow rate can be calculated by the following equation.

$$\frac{\mathrm{dm}}{dt} = \mathrm{V}\frac{d\rho}{dt} = \frac{V}{a^2}\frac{dP}{dt} \text{ (eq-1)}$$

Where $\frac{\mathrm{dm}}{dt}$ is the injected mass flow rate, V is the fixed volume of the measuring chamber, $\rho$ is the density of the fuel, $a$ is the speed of sound measured by the ultrasonic sensor, and P is the chamber pressure. The thermo-regulator integrated in HDA allowed controlling the measurement system temperature, including the injector and fuel temperatures. The pressure of the main chamber is controlled by pressure regulating valves installed in the chamber and the chamber pressure (back-pressure from the perspective of injector) was set to15 bar for all experimental conditions. This is higher than the ambient pressure condition of GDI engine with normal early injection timing as well as the lowest operative chamber pressure of HDA. However, the value was chosen to minimize test errors and

https://doi.org/10.1016/j.fuel.2021.122569

noise caused by cavitation generated by high velocity fuel injection as reported in the earlier study on Zeuch method ROI characterization [31]. In additions, it was reported in in the earlier studies [24] [32] that effect of back pressure on ROI is relatively small while ROI is mainly affected by the square root of the pressure difference across nozzle.

The test conditions are summarized in Table 3.. The duration of injection command pulse (coil energizing time) was varied between 200 μs, the shortest pulse width that fuel can be injected , and 5 ms which is the usual maximum injection duration in a GDI engine considering the intake stroke injection at rated rpm. The fuel injection pressure was varied from 50 bar to 380 bar while the back pressure was fixed at 15 bar. It should be noted that the pressure difference across the nozzle which is the value of subtracting the back pressure from the injection pressure, will be the discussed as an important injection factor in this study. Fuel temperature was varied from 25 ℃ to 100 ℃. In order to characterize the ROI of the injector in practical for the purpose of engine development and calibration, it is very important to perform the measurement at a temperature as low as -30 C, where the viscosity of the fuel increases significantly. However, in this study, the test could not be performed at a temperature lower than the room temperature due to the limitations of the test equipment and facility.

Combining the conditions described above, experiment was conducted for a total of 570 conditions. Fig. 4 shows the summarized test conditions. The fuel was injected at 2 Hz repetition rate and the ROI data were acquired with a sampling rate of 100 kHz. The data were acquired for 100 injections and the ensemble-averaged data were post-processed by noise filtering. Measured ROI data using Zeuch method can be contaminated by measurement errors and noise due to pressure fluctuations in the fuel chamber and mechanical vibrations of the injection system. In particular, high-frequency noise has been reported and measures for noise filtering has been applied to improve signal quality in earlier studies [30] [31]. In this study, moving averaging over 9 consecutive data points was applied considering capability of effective noise reduction and retaining of sharp step response as well as its simplicity and ease of implementation.

### 2.3. **Machine-learning methodology and computational setup**

In the present work, a machine learning function installed in the MATLAB program was utilized as a mean of regression to predict fuel injection rate and solenoid voltage signal. A built-in ANN code using the Bayesian regularization algorithm was applied, following the schematic diagram shown in Fig. 5. The Bayesian regularization

is a mathematical process that converts a nonlinear regression into a "well-posed" statistical problem in the manner of ridge regression. This algorithm is known to be more robust than standard back-propagation methods because it can reduce the need for a lengthy cross-validation process. Thus, it is one of the commonly used algorithms for engineering problems. The building block of an ANN is the layers and neurons that represent the smallest processing element [33][34]. In the neuron, it can have one or more inputs of $x_i$, which comes from the environment or other neurons. These inputs then are multiplied with a weight $w_i$ and are shifted by a bias $w_0$ to provide the intermediate value of y as presented in the following equation, eq-2.

$$y = \sum_{i=1}^{N} w_i x_i + w_0 \text{ (eq-2)}$$

The y from each neuron is transferred through an activation function to provide the output. The activation function can be in various forms such as linear, Gaussian, Heaviside, ramp, or sigmoid. In the present work, sigmoid is used as an activation function for all hidden layers and linear the output layer because it demonstrated the best performance both in terms of prediction and training. As described above, the training on measured ROI and solenoid voltage was performed using 4 inputs such as the pressure drop across the nozzle [bar], the coil energizing time (injection command pulse) [μs], fuel temperature [℃], and Qstat [g/min] with 100 iterations. The output size was 500 by 1 column that covers 0 to 5 ms after the start of the coil energizing time. It was essential to perform the so-called training where the weights and biases of all involved neurons are determined before using the ANN. This task was carried out as an optimization process to minimize the error in predicting the desired output for the input vector of a known dataset. Different combinations of dataset ratios for training, validation, and testing were explored. The best performance was found in 70%, 20%, 10%, and 60%, 20%, 20% for injection rate and solenoid voltage, respectively. Meanwhile, a parametric investigation showed the best agreement with 2 layers that have 10 and 30 neurons, 2 layers that have 9 and 10 neurons for injection rate and solenoid voltage, respectively. Considering the trend of injection quantity and the number of training set, ROI data sets were divided into 4 parts based on the coil energizing time of 0-300μs, 300-700μs, 700-2000μs, and 2000-5000μs regimes. One set was assigned for the ballistic region with energizing time less than 300μs for to predict accurately its injection quantity feature. Another set was assigned for the energizing time from 300μs where ballistic region ends to 700μs which correspond the induced time of the peak current. This was applied to reflect the slight difference in ROI depending on whether the holding phase was applied. For longer energization times with the holding phase, no particular trend is observed except for clear proportional increase with

https://doi.org/10.1016/j.fuel.2021.122569

energization time. However, in the case of the longer energizing time than 2000μs, less measurements were conducted compared to other test conditions due to its linearity. Therefore, a separate regime was assigned for energizing time longer than 2000μs.

## 3. Results and discussion

### 3.1 Discussions on ROI and solenoid voltage measurement results

In this section, the detailed characteristics of measured ROI and solenoid voltage signal will be discussed. Fig. 6 shows the ROI trend according to the coil energizing time. It is shown that trend of ROI is not consistent with the energizing time and it can be divided into three regimes showing distinct characteristics. Region A shown in Fig. 6 is known as the ballistic region. In this region, needle motion follows a parabolic trajectory without reaching the upper position due to the short energizing time [10]. The duration and the amplitude of the ROI increase linearly with energizing time in this region. However, with increasing energizing time, the ROI shows less change, identified as region B in Fig. 6. In this region, the needle lift approaches the mechanical limit therefore, even if the energizing time increases, the needle lift barely changes while the bouncing motion of the needle can occur. As a result, the actual injection quantity does not increase with the increased energizing time while non-linearity of injection quantity arises due to the dynamic behavior of the needle motion as depicted in Fig. 1. On the other hand, with the further increase in coil energizing time, the needle reaches the maximum lift and maintains its position till the end of the coil energizing time. Thus, the injection quantity increases as the energizing time increases again. The relatively proportional relationship between the energizing time and the injection quantity is observed in this region. This corresponds to ‘linear’ region C in Fig 6. As discussed so far, the injection rate shows a distinguishable behavior according to the coil energizing time and injection pressure. It will be evaluated whether the regression model can reflect these behaviors seen in the measurement results.

Fig. 7 shows the effect of pressure difference across the nozzle on ROI. As the pressure difference increases, the peak ROI increases and the ramp during start and end of injection has a higher slope. In particular, the fast ramp-down slope shorten the closing period and the end of injection. However, this trend is shown under Region C conditions of longer coil energizing time where the needle lift reaches its maximum limit. A more complex tendency can be shown when short energizing time is applied. An example is illustrated in Fig. 8 where the ROIs were obtained for various pressure difference with the coil energizing time of 250μs. It is confirmed in Fig.8 that the valve closing delay

decreases as the pressure difference increases from 200 to 350 bar. However, the valve closing delay increases when the pressure difference increases from 100 to 200 bar. Similar trends were also shown in different injectors with a shorter energizing time. Such behavior is the manifestation of non-monotonic effect of pressure difference during the valve closing period. In general solenoid type GDI injectors, if the pressure difference is high, the hydraulic force of the pressurized fuel pressing the needle ball increases as presented in earlier study [35]. As a result, the needle descends towards the seat faster, shortening the closing delay. However, if there is no effect of accelerating the closing motion of the ball and needle by the pressurized fuel, ROI will only depend on the pressure difference and fixed effective area of the nozzle. As a result, the closing delay can increase as the pressure difference increases. Under the condition of a short energizing time near the ballistic region and some pressure difference condition, the energizing time ends when the needle lift is small and the hydraulic force due to pressurized fuel is small compared to the spring force. As a result, higher pressure difference can increase the valve closing delay as shown in Fig. 8. The non-monotonic trend observed for the relationship between pressure difference and valve closing delay will be included in a checklist for the verification of the model's accuracy.

Fig. 9 shows the impact of fuel temperature on ROI. The slight decrease of the peak ROI can be seen with higher temperature, even though the difference is almost negligible. The valve opening and closing delay were also slightly reduced as the temperature increased. This is because of density and viscosity decrease as the fuel temperature increases, reducing the friction that the needle motion is subject to. It is worthwhile to reiterate that the ROI test was not performed under very cold conditions below zero such as -30 degrees, where the viscosity of the fuel increases significantly [36][37]. Therefore, the influence of fuel temperature was shown to be very small and the accuracy and the importance of the modeling is expected to be relatively low if it were to extrapolate to cold temperature conditions. However, as one of the test conditions, an evaluation will be performed to check if the model can predict the effect of fuel temperature on ROI to be small as shown in the experimental results.

As an additional piece of ROI modeling, the effect of the static flow rate of each injector on the ROI is shown in Fig. 10. It can be seen that the maximum injection flow rate increases linearly as the static flow rate increases as expected. Five injectors having different Qstat as shown in the table were tested in the study, and it will be discussed later whether the model can predict the ROI trend according to the Qstat in the model validation section.

https://doi.org/10.1016/j.fuel.2021.122569

Fig. 11 shows the correlation between the timing when inflection point in the solenoid voltage signal is observed and the actual EOI timing calculated from ROI. The inflection point of the solenoid voltage shown in Fig. 11 was found as the value at which the second derivative of injection driving voltage became zero. This is the method that was applied to the actual logics in engine control unit (ECU) as shown in earlier study [12] even more advanced methods are now applied to reduce errors and variations. In Fig. 11, it is confirmed that the inflection point of the solenoid voltage and actual EOI timing have a strong correlation as explained in the introduction. If the ROI and solenoid voltage can be accurately predicted through regression modeling, it will be possible to develop, validate and pre-calibrate the injection control logic in ECU using these models for a virtual development environment. The possibility will be discussed later in the model validation section.

### 3.2. Regression model development and evaluation

To validate the model, the correlation between the predicted data from the ANN and experimental data was evaluated for both ROI and solenoid voltage models. Table 4 shows the $R^2$ for all of the training, validation, and test data sets for the model. Both models show a high $R^2$ which indicates the quality of regression is sufficient to make a prediction for ROI and solenoid voltage signal. Most of the training score reached over 0.99 except for the short energizing time (0-300μs) case due to the inherent non-linearity in ROI discussed in the previous section. This shows that superior accuracy of the model could be achieved compared to the previous study previous study that performed 1D hydraulic simulations on a GDI injector and reported an R2 of 0.92 under linear injection quantity condition [22]. Other than the training data set, new inputs that were not even included in the training, validation, and test procedure were tested as shown in Fig. 12. The comparison between ROI prediction by the machine-learning algorithm and experimental result indicates the models can predict ROI features of not only quasi steady-state but also transient dynamics. The machine-learning algorithm is able to detect SOI, and EOI precisely by showing closely matching those timings with the experimental result regardless of injectors' pressure difference, coil energizing time, fuel temperature, and static flow rate. The details of ROI, for example, decrease in ROI during needle lift-up, fluctuations in early injection period, and even after needle close were well replicated with the machine-learning algorithm. Again, it is emphasized that the conditions in Fig. 12 were excluded in any training dataset but utilized for the evaluation of the models.

### 3.3. Model validation and discussions

https://doi.org/10.1016/j.fuel.2021.122569

Comparison of the injection quantity calculated by integrating ROI trace for both model and experimental result is shown in Fig. 13. (a). Experimental symbols shown in Fig.13 (a) may seem insufficient to derive the modeled curve but it can be noted that they are experimental results form injector #1 while the modeled injection quantity curve was derived from the results of 5 different injectors. It can be seen that the model matches well with the experimental results. In particular, it was confirmed that the model can simulate the injection quantity characteristics, which were categorized according to the length of the energizing time. Figure 13 (b) shows ROIs according to various energizing time injection periods for the model and the experiments. In Fig. 13(b), the modeled and measured ROIs almost overlap each other so it is believed that the detail of ROI according to the length of the energizing time could be accurately predicted.

The trend of modeled ROI according to pressure difference across the nozzle for various coil energizing times is shown in Figs. 14 and 15. In particular, Fig. 14 shows the modeled and measured ROIs for the relatively long energizing time of 700μs and the modeled and measured curves almost overlap for various conditions. Therefore, it can be confirmed that accuracy of the prediction is significantly high compared to previous 0D and 1D studies which showed some inconsistency in the valve opening and closing periods for various injection conditions [22][23][25]. In Figs. 14 and 15, The trend observed in the test results is well confirmed in the modeled ROI. In particular, it was shown that the effect of pressure difference on valve closing delay according to the length of the energizing time matched well with the experimental results. In the previous discussion, the effect of the injection pressure on the valve closing delay was identified that it shows different behaviors according to the length of the energizing time. If the energizing time is long enough to have the linearity of the injection quantity, the valve closing delay decreases as the pressure difference increases, while the opposite trend could be shown for the shorter energizing time . The accurate modeling of these complex effects was possible as shown in Fig. 15. Some modeled ROI cases showed a slight quantitative difference with the measured ROI near the end of injection timing, particularly for short events, but the overall trend and injected mass matches well with the experimental results. In particular, it can be confirmed that the accuracy and effectiveness of the approach in this study is superior compared to the 1D and 0D models in the previous studies, which had difficulties in modeling or scored low accuracy in the ballistic region [23][25].

As discussed in the previous experimental results section, as the injector temperature increases, the injection rate is slightly decreased due to the decreased fuel density, and the decreased viscosity decreases the delay of valve closing

and opening. The ROI model shown in Fig.16 follows these trends. Although the model was developed from relatively smaller number of fuel temperature tests, reliable predictions are shown at intermediate temperatures with no evidence of overfitting, including conditions excluded from the training dataset.

Figure 17 shows the modeled ROI according to the static flow rate of the injector. Comparing the test results and the modeled prediction, it was confirmed that the trend of ROI for the static flow rate was predicted very accurately and the measured and predicted curves almost overlap in Fig. 17. In addition, the model could provide an appropriate prediction without overfitting or misbehavior under conditions where the experiments were not carried out. This indicates that the approach introduced in this study can be used not only to develop a model for a particular injector but also as a universal injector model applicable to the nominally identical injector family that have deviations from designed flow rates. This is a feature that is considered to be very useful in a virtual development environment.

A comparison of the measured solenoid voltage signal and the virtual signal generated by the regression model is shown in Fig. 18 (a). As shown in the figure, the solenoid voltage signal can be predicted accurately through the modeling described in 2.2. In particular, the inflection point of the modeled voltage signal is close to that of the measured voltage. A key outcome of this finding is the modeled voltage is available for verification of injection control logic in the virtual development environment. As discussed previously in Fig. 10, the measured inflection point of the solenoid voltage, or the second derivative of the voltage signal, becomes zero at the actual EOI timing. Fig. 18 (b) shows the first and second-order derivatives of voltage signals from both the measurement result and the model. In Fig. 18(b), it was identified that the same signal processing method can be applied as in the actual ECU. The inflection point of the modeled voltage signal and the identified valve closing delay are close to those of the measured signal. Figure 19 shows the comparison of the EOI timings calculated through the model and measurement results for various test conditions. From Fig. 19, it is confirmed that there is a strong correlation between the EOI timings obtained respectively from the model and the measurement results.

The above discussions show that both the injection rate and the solenoid voltage signal can be modeled with high correlation to the actual measurement result. In addition, it was confirmed that the virtually generated signal can be processed through the same signal processing method which applies to an actual ECU, in the same manner as the actual signal. Therefore, as suggested in the Introduction, the model proposed in this study can be used for the development, verification, and preliminary calibration of ECU injection logic in a virtual development environment.

https://doi.org/10.1016/j.fuel.2021.122569

The actual application of these models in a virtual development environment will be carried out as the authors' future study.

Based on the ML and ANN approach, the models produced demonstrate superior accuracy for predicting ROI and voltage signals, much closer to actual measurement results, than any other modeling techniques introduced in previous studies. In particular, most of the previous studies have reported difficulty in accurate modeling under short energizing time conditions in which the needle doesn't reach the full lift position during the injection. On the contrary, reliable modeling was possible even under such conditions in this study using ML and ANN. Since these conditions are regarded as the most important conditions in actual engines for realizing reliable and repeatable application of injection strategy, the usefulness of the proposed approach in this study can be recognized.

The modeling proposed in this study has the disadvantage that it depends completely on experimental ROI data. Also, unlike CFD prediction, it can't provide referenceable results other than preset output values. Therefore, the approach proposed in this study won't be suitable for the fundamental injector researches to understand the injection phenomenon and analyzes the detail of spray characteristics. On the other hand, this approach will be suitable for agile modeling for practical engine development. In particular, it is believed that engineers performing these tasks have already have accumulated test results of ROI and solenoid signals for the previous injection control logic development and calibration. Therefore, it is believed that the simple and accurate ROI and solenoid signal models can be developed using the methodology introduced in this study based on the existing injection data and utilized for the virtual powertrain development.

## 4. Conclusion

In this study, a machine-learning algorithm was implemented to predict injection rate of the state-of-the-art GDI injectors. Experimental data measured under various injection conditions were utilized for algorithm training. The major findings from this study can be summarized as follows.

1) Rate of injection (ROI) measurement confirmed the non-linear behavior of fuel injection rate according to coil energizing time and pressure difference across the nozzle. Near the ballistic region, the injection quantity did not increase with longer coil energizing time while a stagnation point was observed. In addition, end of injection

(EOI) were advanced with higher pressure difference in the general manner while non monotonic trend was shown under some conditions due to complex effects of pressure difference on internal flow and needle behavior.

2) Simple regression model without time-marching simulation using the artificial neural network (ANN) technique was developed in this study. The model was able to capture detailed characteristics in rate of injection (ROI) and solenoid voltage signal with 4 input features, pressure difference, coil energizing time, fuel temperature and static flow rate of the injector respectably. The model has significantly reduced requirements for input information and computational resource compared to CFD approach.
3) The ANN model showed also advantages on the accuracy of the prediction. Despite non-linear characteristics in the injection rate, the training showed high coefficient of determination over 0.975. The quantitative comparison between machine-learning model and experimental data showed that the ANN model is capable of predicting not only general features of the injection rate trend but also non-linear behaviors shown in ROI measurement results.
4) The end of injection (EOI) could be detected precisely with virtually generated solenoid voltage signal and same signal processing method which applies to an actual engine control unit. Correlation between the detected EOI timings calculated from the modeled signal and the measurement results showed the very high coefficient of determination of 0.998. The ROI and solenoid voltage model developed in this study is enough to be utilized for the development, verification, and pre-calibration of the injection control logic in a virtual powertrain development environment.

**Acknowledgements**

The authors would like to thank Logan White, Aaron Czeszynski, Nathan Harry and Steve Busch for their kind support on this study. The authors also thanks to Namho Kim for his valuable feedback on the manuscript.

Financial support for this study was provided by Hyundai Motor Company under an agreement ‘FI083200616A’ with Sandia National Laboratories. Hyundai Motor Company also supported an international visiting program of Heechang Oh at Sandia National Laboratories under agreement ‘FI083200616-0’.

All of the experimental work was performed at the Combustion Research Facility (CRF), Sandia National Laboratories, Livermore, CA, United State of America. Sandia National Laboratories is a multi-mission laboratory managed and operated by National Technology and Engineering Solutions of Sandia, LLC., a wholly owned

subsidiary of Honeywell International, Inc., for the U.S. Department of Energy's National Nuclear Security Administration under contract DE-NA0003525.

**CRediT authorship contribution statement**

Heechang Oh: Conceptualization, Investigation, Writing - original draft.

Joonsik Hwang: Conceptualization, Investigation, Writing - original draft.

Lyle M. Pickett: Writing - review & editing, Supervision.

Donghee Han : Writing - review & editing, Supervision.

**Declaration of Competing Interest**

The authors declare that they have no known competing financial interests or personal relationships that could have appeared to influence the work reported in this paper.

**References**

[1] Energy Technology Perspectives 2020. Energy Technol Perspect 2020 2020. https://doi.org/10.1787/ab43a9a5-en.

[2] Hyundai. Road to Sustainability 2020 2020:1–125.

[3] Wukisiewitsch W, Danzer C, Semper T. Systematical Development of Sustainable Powertrains for 2030 and Beyond. MTZ Worldw 2020;81:30–7. https://doi.org/10.1007/s38313-019-0162-5.

[4] Kaita, K. Diversified Electrification – The Key for Toyota's Challenge towards a Sustainable Society. 40th International Vienna Motor Symposium, 15 to 17 May 2019, VDI Wien, 2019.

[5] Reitz RD, Ogawa H, Payri R, Fansler T, Kokjohn S, Moriyoshi Y, et al. IJER editorial: The future of the internal combustion engine. Int J Engine Res 2020;21:3–10. https://doi.org/10.1177/1468087419877990.

[6] Yu C, Park K, Han S, Kim W. Development of theta II 2.4L GDI engine for high power & low emission. SAE Tech Pap 2009. https://doi.org/10.4271/2009-01-1486.

[7] Kim D, Rao L, Oh H, Kook S. In-cylinder flow structure of a production spark-ignition engine at cold start

conditions 2020. https://doi.org/10.14264/63c65e8.

[8] Downsizing in the High Performance Segment - Not a Contradiction in Terms for AMG! The New V8 Engine Family from AMG, 23rd Aachen Colloquium Automobile and Engine Technology 2014 2014:2014.

[9] Targets D. The New 1 . 5-l Four- cylinder TSI Engine from Volkswagen 2017:16–23.

[10] Parotto M, Sgatti S, Sensi F. Advanced GDI injector control with extended dynamic range. SAE Tech Pap 2013;2. https://doi.org/10.4271/2013-01-0258.

[11] Taglialatela Scafati F, Pirozzi F, Cannavacciuolo S, Allocca L, Montanaro A. Real Time Control of GDI Fuel Injection during Ballistic Operation Mode. SAE Tech Pap 2015;2015-September. https://doi.org/10.4271/2015-24-2428.

[12] Sun P, Xin B, Wang X, Zhang H, Long L, Wang Q. Research on correction of flow characteristics in ballistic zone of GDI engine injector. 2020 4th CAA Int Conf Veh Control Intell CVCI 2020 2020:324–9. https://doi.org/10.1109/CVCI51460.2020.9338643.

[13] Hammer J, Kufferath A, Wehmeier K. Modern GDI combustion systems with focus on fuel metering technology fulfilling future emission legislation. SIA-The spark ignition engine of the future, 2011.

[14] Piock W, Hoffmann G, Spakowski J, Dober G, Gomot B, Hulser H. Delphi Technologies Next Generation GDI system – improved Emissions and Efficiency with higher pressure. 40th International Vienna Motor Symposium, 15 to 17 May 2019, VDI Wien, 2019

[15] Barasa P, Tian Y, Hardes S, Owlia S, Limaye P, Bailey D, et al. Virtual Engine, Controls, and Calibration Development in Automated Co-Simulation Environment. SAE Tech Pap 2016. https://doi.org/10.4271/2016-01-0090.

[16] Dorscheidt F, Düzgün M, Claßen J, Krysmon S, Pischinger S, Görgen M, et al. Hardware-in-the-Loop Based Virtual Emission Calibration for a Gasoline Engine. SAE Tech Pap 2021. https://doi.org/10.4271/2021-01-0417.

[17] Fan S, Sun Y, Lee J, Ha J. A Co-Simulation Platform for Powertrain Controls Development. SAE Tech Pap 2020;2020-April:7191. https://doi.org/10.4271/2020-01-0265.

[18] Baldwin E, Grover R, Parrish S, Duke D, Matusik K, Powell C. String flash-boiling in gasoline direct injection simulations with transient needle motion. Int J Multiph Flow 2016;87:90–101. https://doi.org/10.1016/j.ijmultiphaseflow.2016.09.004.

[19] Xue Q, Battistoni M, Powell CF, Longman DE, Quan SP, Pomraning E, et al. An Eulerian CFD model and X-ray radiography for coupled nozzle flow and spray in internal combustion engines. Int J Multiph Flow 2015;70:77–88. https://doi.org/10.1016/j.ijmultiphaseflow.2014.11.012.

[20] Payri R, Tormos B, Salvador FJ, Plazas AH. Using one-dimensional modelling codes to analyse the influence of diesel nozzle geometry on injection rate characteristics. Int J Veh Des 2005;38:58–78. https://doi.org/10.1504/IJVD.2005.006605.

[21] Kim J, Lee J, Kim K. Numerical study on the effects of fuel viscosity and density on the injection rate performance of a solenoid diesel injector based on AMESim. Fuel 2019;256:115912. https://doi.org/10.1016/j.fuel.2019.115912.

[22] Lee K, Kim N, Cho Y,Lee Dm Park S. Modeling Dynamic Behavior and Injection Characteristic of a GDI Injector, Journal of ILASS-Korea 2017:22(4):210–217. https://doi.org/10.15435/JILASSKR.2017.22.4.210

[23] Postrioti L, Cavicchi A, Paolino D, Guido C, Parotto M, Di Gioia R. An experimental and numerical analysis of pressure pulsation effects of a Gasoline Direct Injection system. Fuel 2016;173:8-28. https://doi.org/10.1016/j.fuel.2016.01.012

[24] Payri R, Gimeno J, Novella R, Bracho G. On the rate of injection modeling applied to direct injection compression ignition engines. Int J Engine Res 2016;17:1015–30. https://doi.org/10.1177/1468087416636281.

[25] Payri R, Bracho G, Gimeno J, Bautista A. Rate of injection modelling for gasoline direct injectors. Energy Convers Manag 2018;166:424–32. https://doi.org/10.1016/j.enconman.2018.04.041.

[26] Hwang J, Lee P, Mun S, Karathanassis IK, Koukouvinis P, Pickett LM, et al. Machine-learning enabled prediction of 3D spray under engine combustion network spray G conditions. Fuel 2021;293:120444. https://doi.org/10.1016/j.fuel.2021.120444.

[27] Ikeda Y, Mazurkiewicz D. Application of neural network technique to combustion spray dynamics analysis. Lect Notes Comput Sci (Including Subser Lect Notes Artif Intell Lect Notes Bioinformatics) 2002;2281:408–25. https://doi.org/10.1007/3-540-45884-0_30.

[28] Zhang Y, Xu S, Zhong S, Bai X-S, Wang H, Yao M. Large eddy simulation of spray combustion using flamelet generated manifolds combined with artificial neural networks. Energy AI 2020;2:100021. https://doi.org/10.1016/j.egyai.2020.100021.

[29] Koukouvinis P, Rodriguez C, Hwang J, Karathanassis I, Gavaises M. International Journal of Engine Research , 2021 Machine Learning and supercriticaltranscritical sprays : a demonstration study of their potential in ECN Spray-A n.d.

[30] Busch S, Miles PC. Parametric Study of Injection Rates With Solenoid Injectors in an Injection Quantity and Rate Measuring Device. J Eng Gas Turbines Power 2015;137:1–9. https://doi.org/10.1115/1.4030095.

[31] Takamura A, Ohta T, Fukushima S, Kamimoto T. A Study on Precise Measurement of Diesel Fuel Injection Rate. SAE Tech Pap 1992. https://doi.org/10.4271/920630.

[32] Vass S, Németh H. Sensitivity Analysis of Instantaneous Fuel Injection Rate Determination for Detailed Diesel Combustion Models. Period Polytech Transp Eng 2013;41:177-85. https://doi.org/10.3311/PPtr.7106

[33] Fernandes de Mello R, Antonelli Ponti M. Machine Learning: A Practical Approach on the Statistical Learning Theory. Mach Learn 2018:373.

[34] Alpaydin E. Introduction to machine learning - third edition, The MIT Pres, 2014.

[35] Chang M, Kim H, Park J, Wang J, Park S. Ball Motion and Near-Field Spray Characteristics of a Gasoline Direct Injection Injector using an X-ray Phase-Contrast Imaging Technique under High-Injection Pressures. Int. J. Heat Mass Transf. 2021;166:120725. https://doi.org/10.1016/j.ijheatmasstransfer.2020.120725

[36] Hwang J, Park Y, Bae C, Lee J, Pyo S. Fuel temperature influence on spray and combustion characteristics in a constant volume combustion chamber (CVCC) under simulated engine operating conditions. Fuel 2015;160:424–33. https://doi.org/10.1016/j.fuel.2015.08.004.

[37] Park Y, Hwang J, Bae C, Kim K, Lee J, Pyo S. Effects of diesel fuel temperature on fuel flow and spray

https://doi.org/10.1016/j.fuel.2021.122569

characteristics. Fuel 2015;162:1–7. https://doi.org/10.1016/j.fuel.2015.09.008.

Table 1. Specification of test injectors

| Injector | Static flow rate [g/min] | Number of holes |
|---|---|---|
| #1 | 415 | 6 |
| #2 | 380 | 5 |
| #3 | 350 | 6 |
| #4 | 270 | 5 |
| #5 | 250 | 6 |

https://doi.org/10.1016/j.fuel.2021.122569

Table 2 properties and components of PACE20, the surrogate fuel for research-grade E10 gasoline

| component | Volume fraction | Property | Specification |
|---|---|---|---|
| ethanol | 0.0955 | Molecular weight | 93.18 |
| n-pentane | 0.1395 | RON | 92.1 |
| cyclopentane | 0.105 | MON | 84.5 |
| 1-hexene | 0.0541 | H:C | 1.964 |
| n-heptane | 0.1153 | Density [g/mL] [3] | 0.742 |
| toluene | 0.0919 | Particulate Matter Index | 1.5 |
| iso-octane | 0.2505 | ASTM D86 T10 [°C] | 57.7 |
| 1,2,4-tri methylbenzene | 0.1187 | ASTM D86 T50 [°C] | 101.4 |
| tetralin | 0.0295 | ASTM D86 T90 [°C] | 158.3 |

https://doi.org/10.1016/j.fuel.2021.122569

Table 3. Experimental conditions

| Parameter | Conditions |
|---|---|
| Injection pressure [bar] | 50-380 |
| Chamber(back) pressure [bar] | 15 |
| Fuel temperature [°C] | 25 - 100 |
| Coil energizing time [μs] | 200 - 5000 |

https://doi.org/10.1016/j.fuel.2021.122569

Table 4. Coefficient of determination for ML algorithms.

| Models | $R^2$ Value |
|---|---|
| ROI $t_{inj} < 0.3ms$ | 0.975 |
| ROI $0.3ms \leq t_{inj} < 0.7ms$ | 0.997 |
| ROI $0.7ms \leq t_{inj} < 2ms$ | 0.997 |
| ROI $2ms \leq t_{inj} < 5ms$ | 0.995 |
| Solenoid voltage | 0.996 |

https://doi.org/10.1016/j.fuel.2021.122569

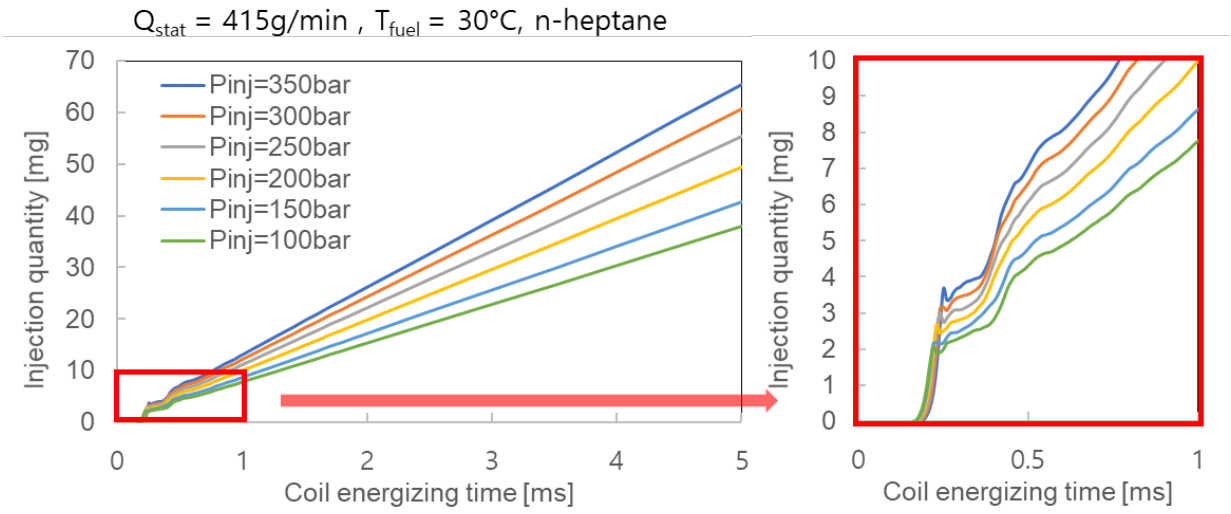


(a) Injection quantity curve and non-linearity

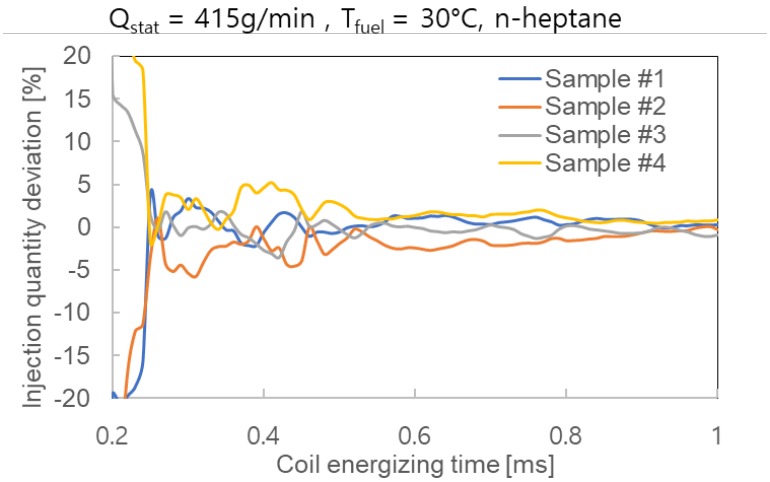


(b) Sample to sample variation

Fig. 1. Injection quantity non-linearity and sample to sample variation of GDI injectors.

https://doi.org/10.1016/j.fuel.2021.122569

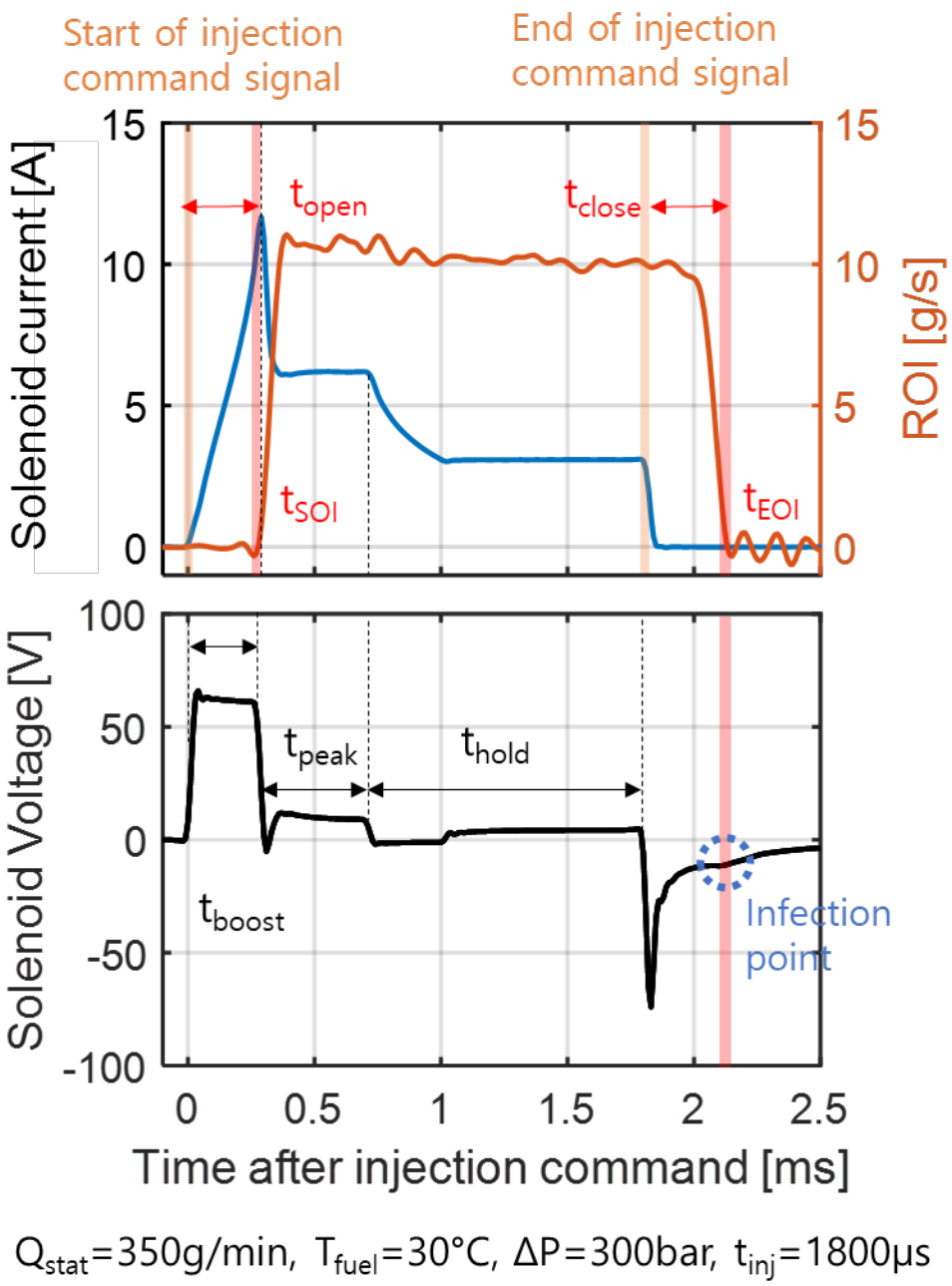


Figure 2. EOI detection using solenoid voltage signal.

https://doi.org/10.1016/j.fuel.2021.122569

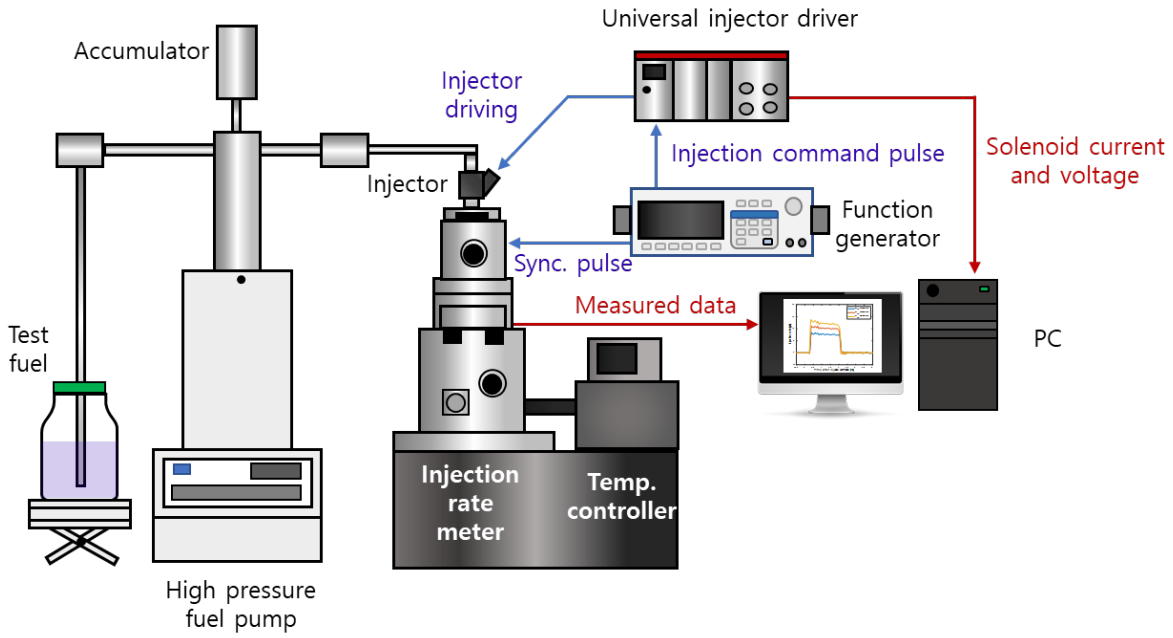


Figure 3. The schematics of ROI measurement.

https://doi.org/10.1016/j.fuel.2021.122569

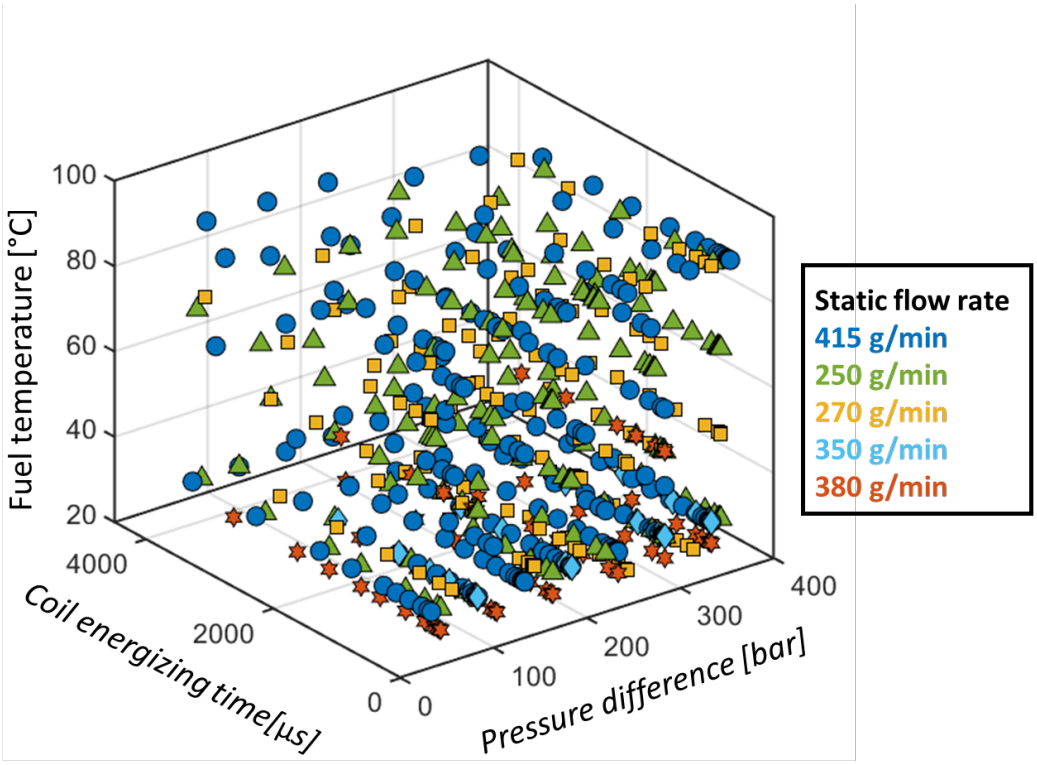


Figure 4. Experimental conditions.

https://doi.org/10.1016/j.fuel.2021.122569

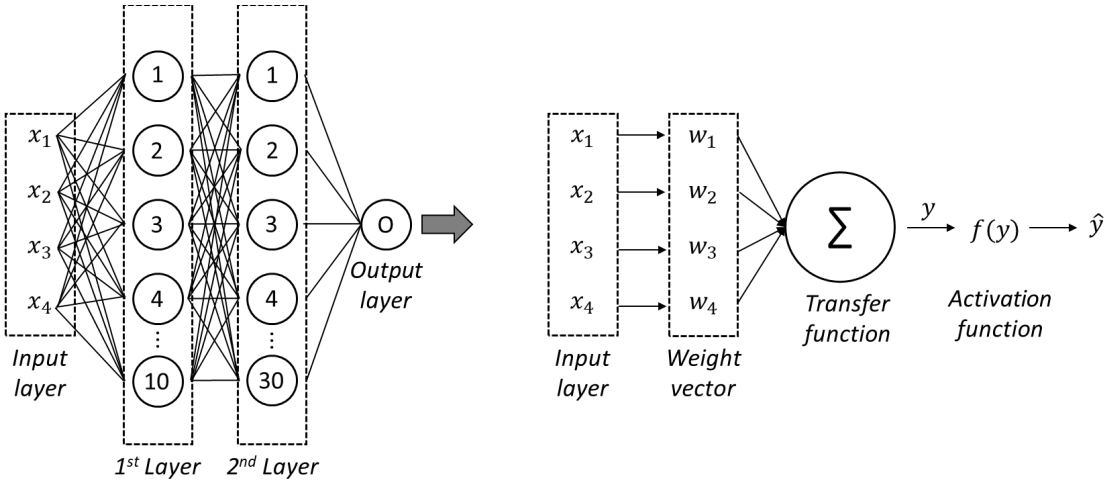


Figure 5. Schematics of regression modeling using artificial neural network .

https://doi.org/10.1016/j.fuel.2021.122569

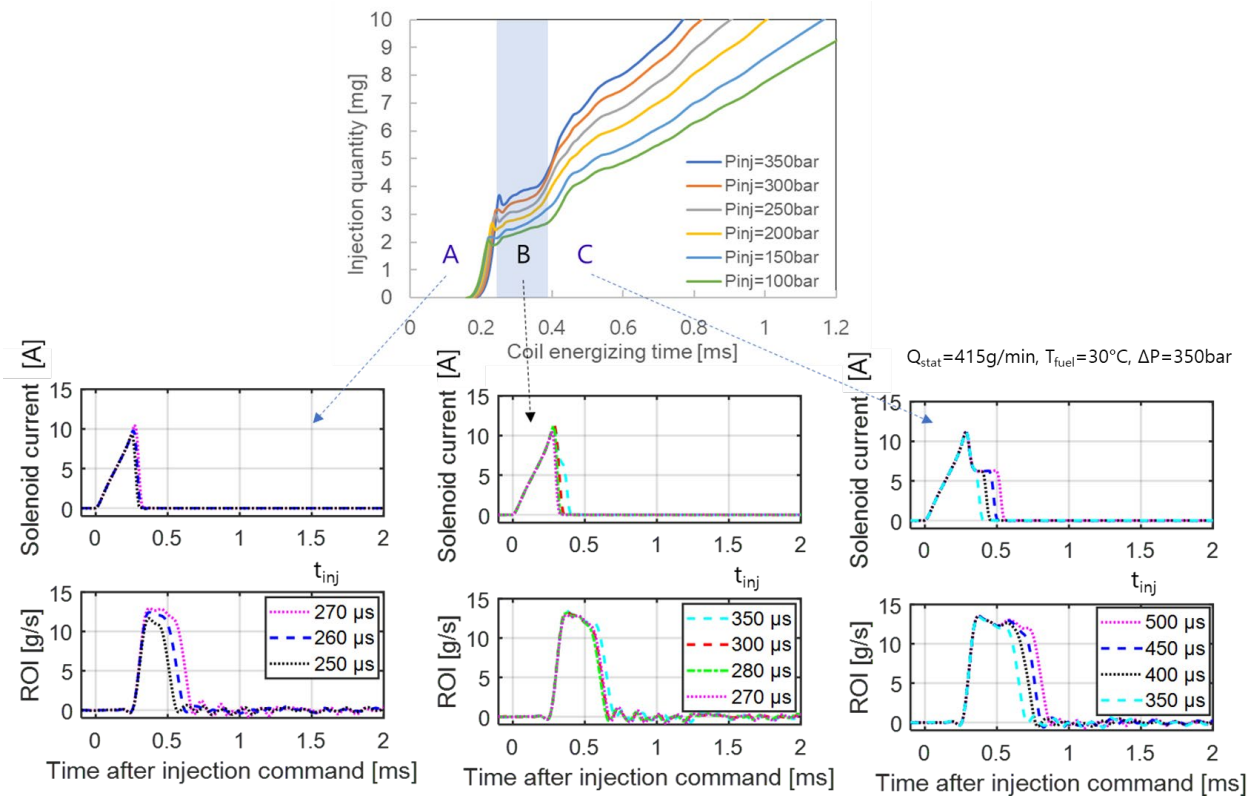


Figure 6. Effect of coil energizing time on ROI and injection quantity.

https://doi.org/10.1016/j.fuel.2021.122569

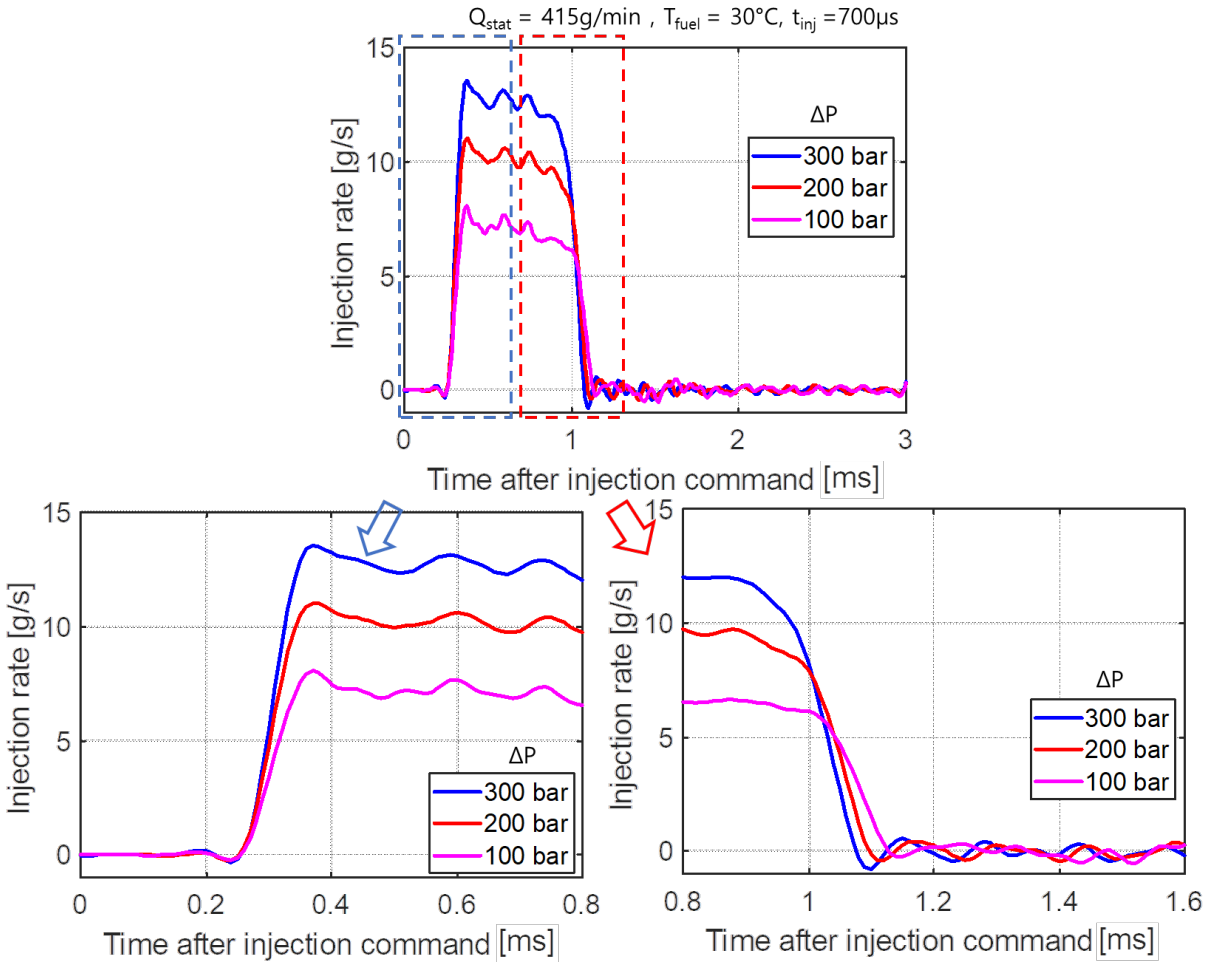


Figure 7. Effect of pressure difference on ROI under longer energizing time condition.

https://doi.org/10.1016/j.fuel.2021.122569

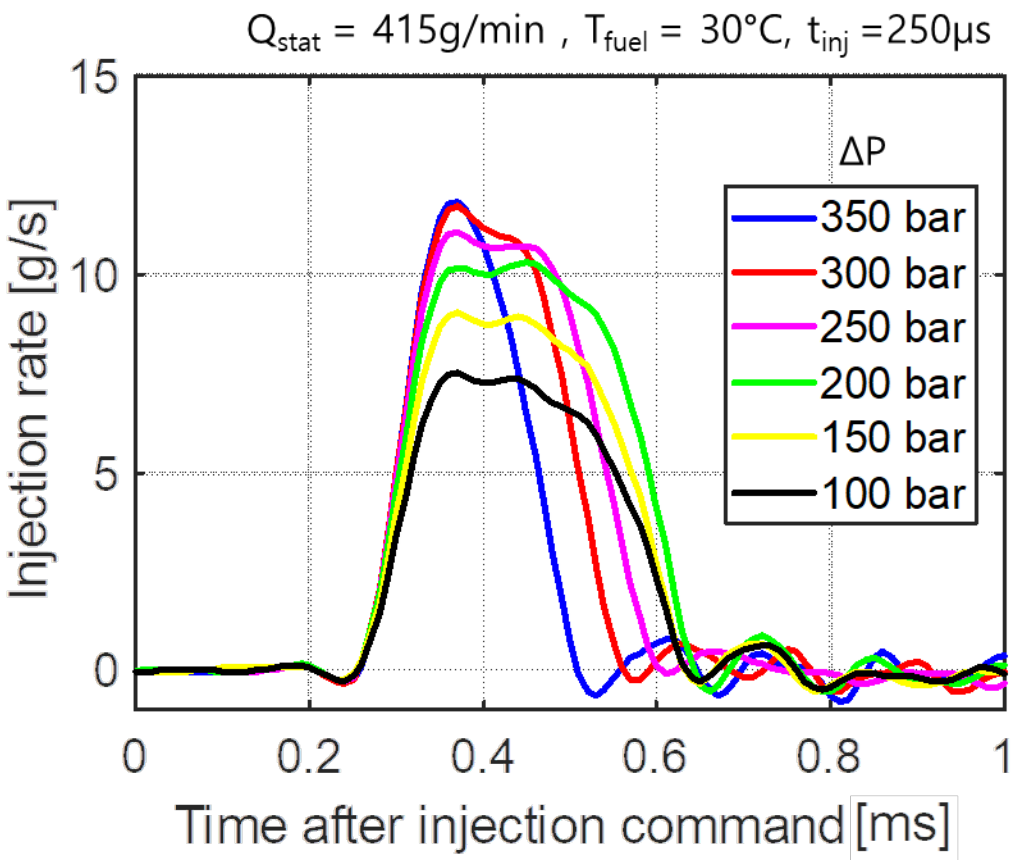


Figure 8. Effect of pressure difference on ROI under longer energizing time condition.

https://doi.org/10.1016/j.fuel.2021.122569

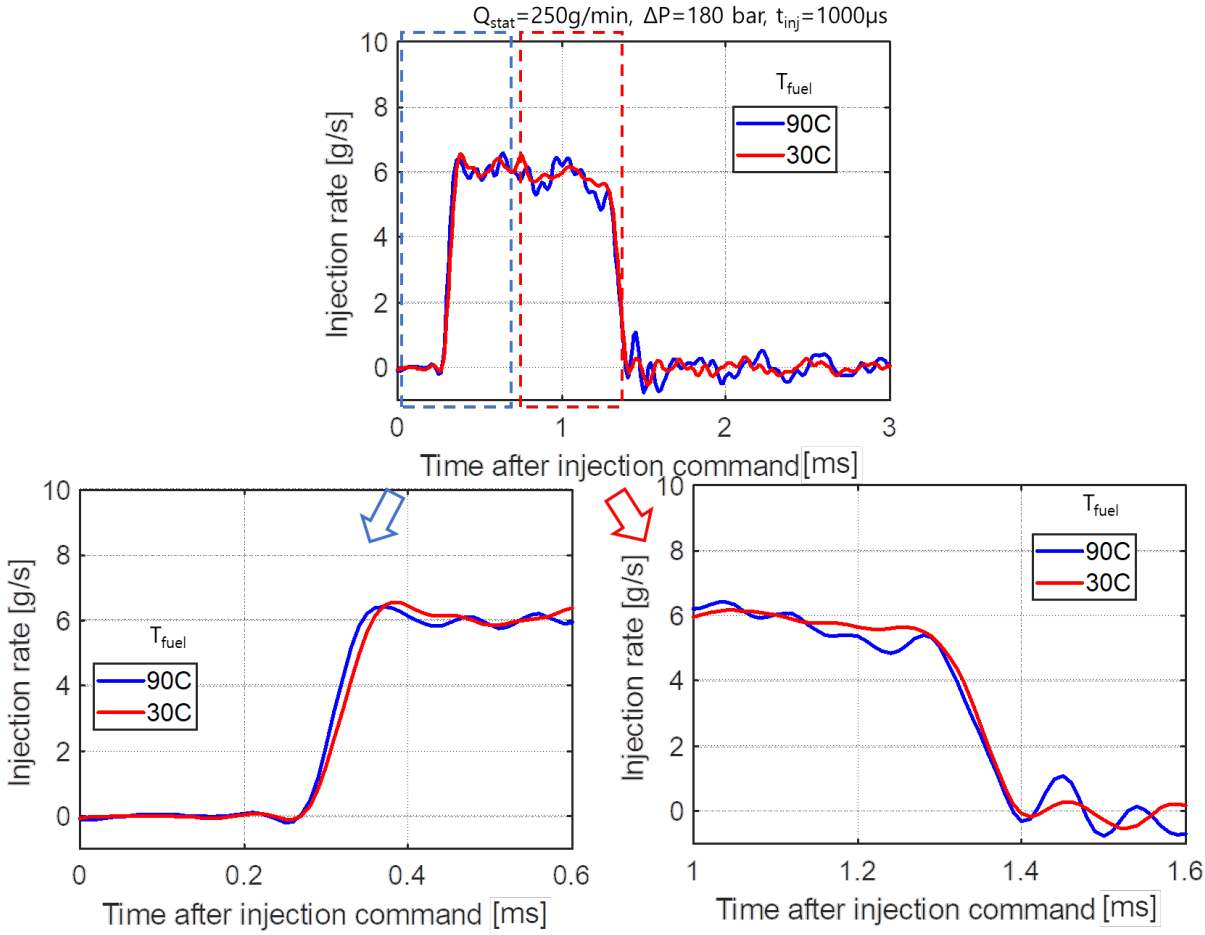


Figure 9. Effect of injector temperature on ROI.

https://doi.org/10.1016/j.fuel.2021.122569

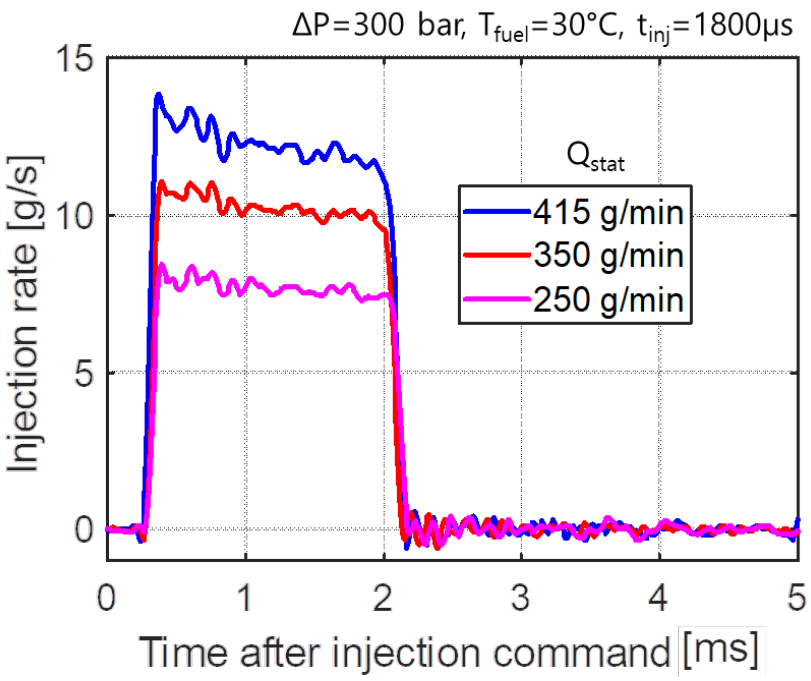


Figure 10. Effect of injector static flow rate on ROI.

https://doi.org/10.1016/j.fuel.2021.122569

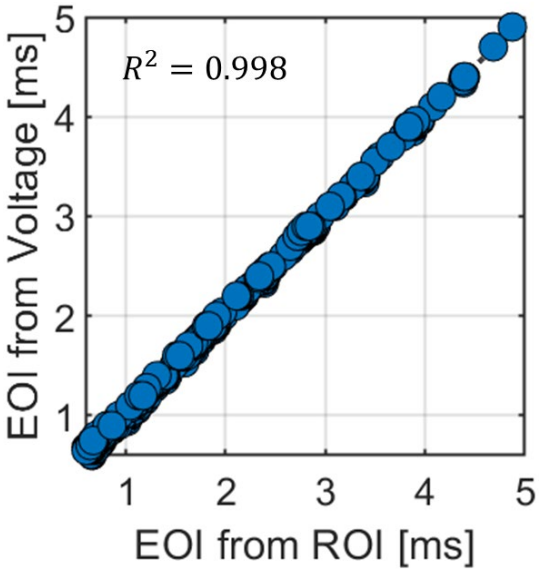


Figure 11 Correlation between end of injection timings calculated from ROI and measured from solenoid voltage signal (all measurement results).

https://doi.org/10.1016/j.fuel.2021.122569

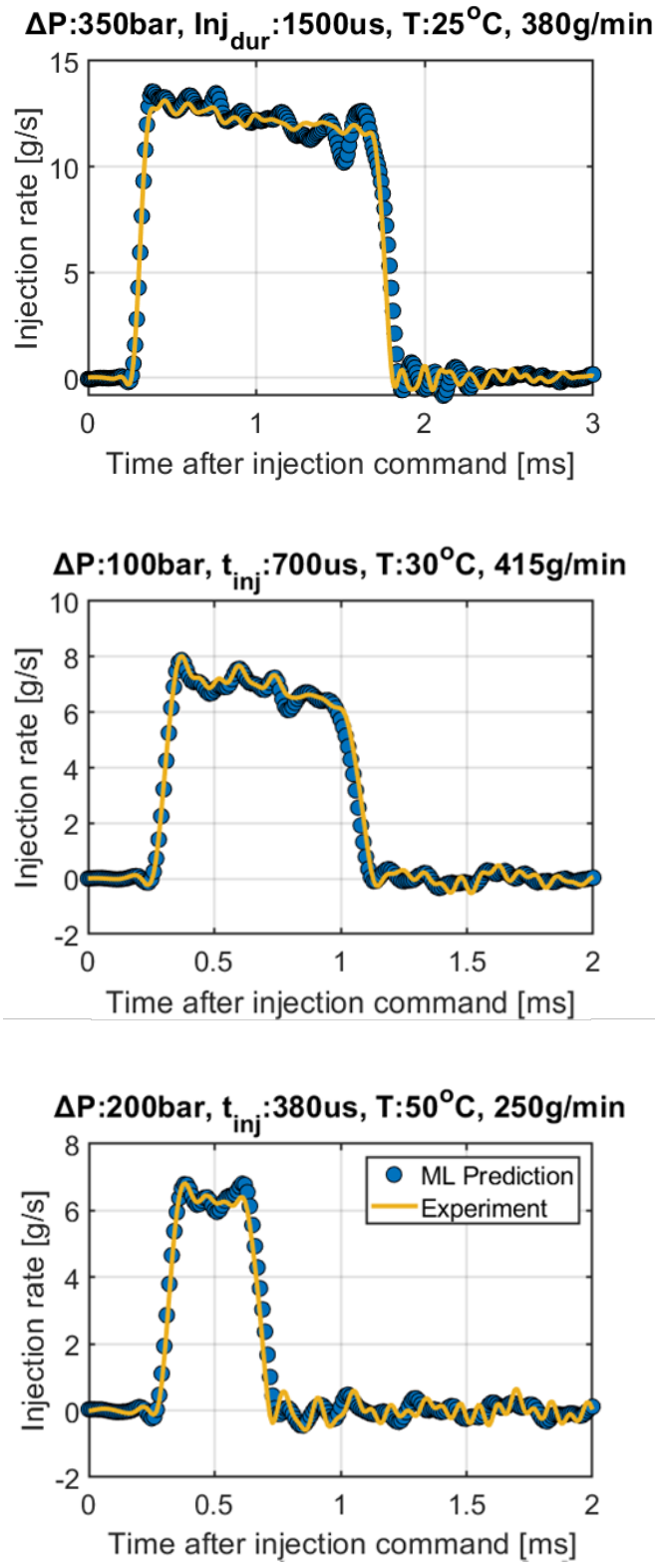


Figure 12. Examples of the modeled ROI and comparison to the experimental results.

https://doi.org/10.1016/j.fuel.2021.122569

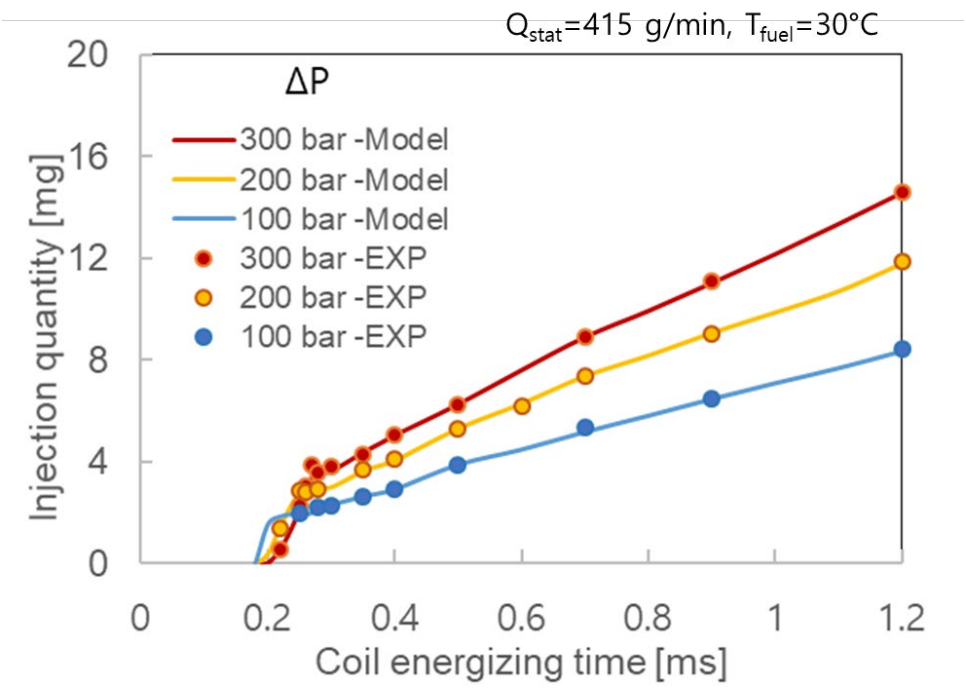


(a) Injection quantity from model and measurement results.

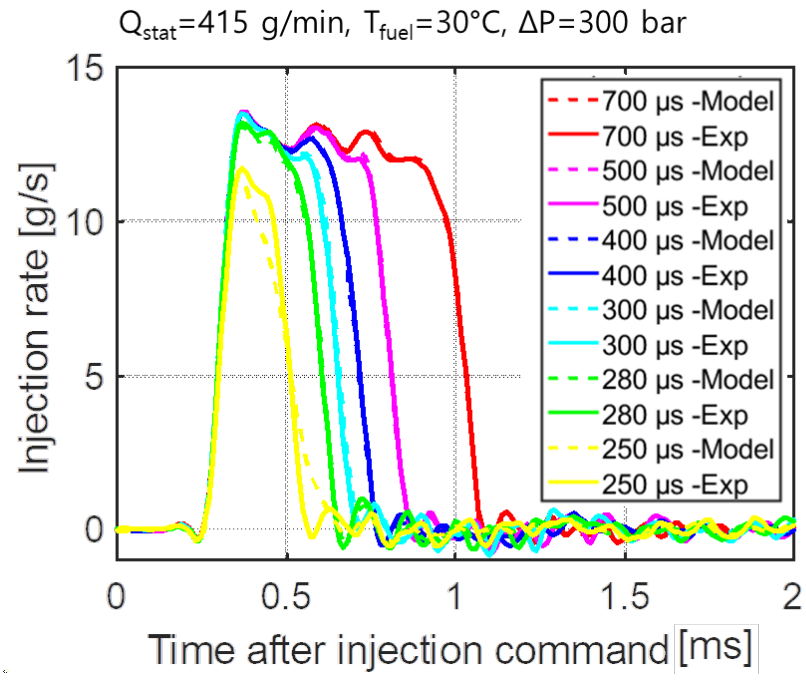


(b) Comparison of ROI.

Figure 13. Comparison of the injection quantity and ROI for model and measurement results.

https://doi.org/10.1016/j.fuel.2021.122569

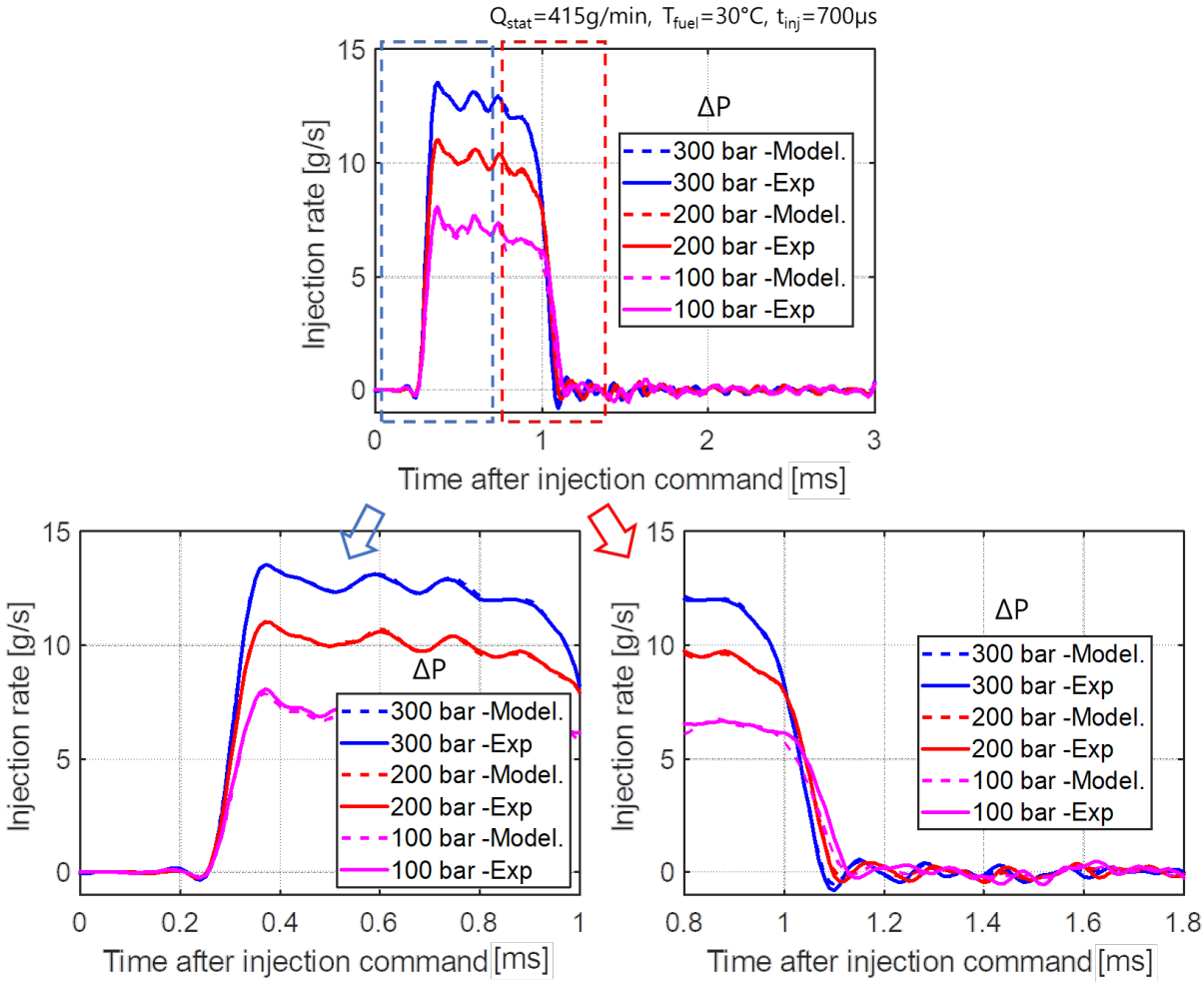


Figure 14. Modeled ROIs for different pressure difference under longer coil energizing time conditions.

https://doi.org/10.1016/j.fuel.2021.122569

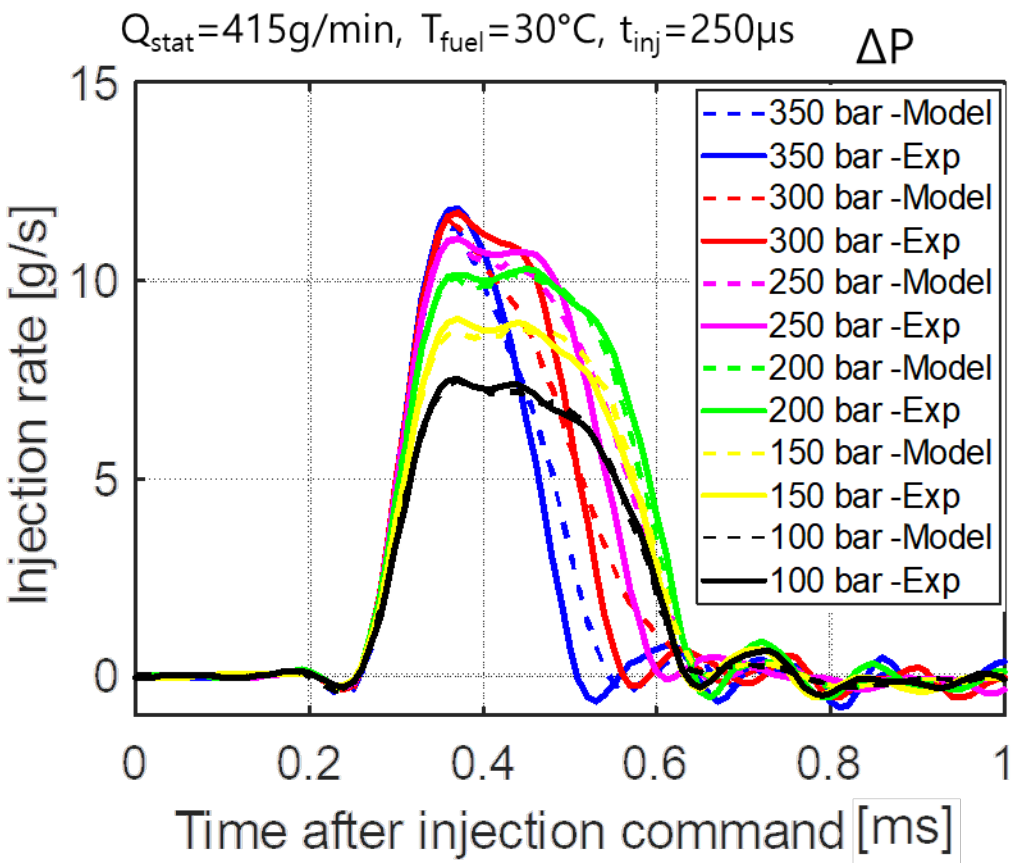


Figure 15. Modeled ROIs for different pressure difference under longer coil energizing time conditions.

https://doi.org/10.1016/j.fuel.2021.122569

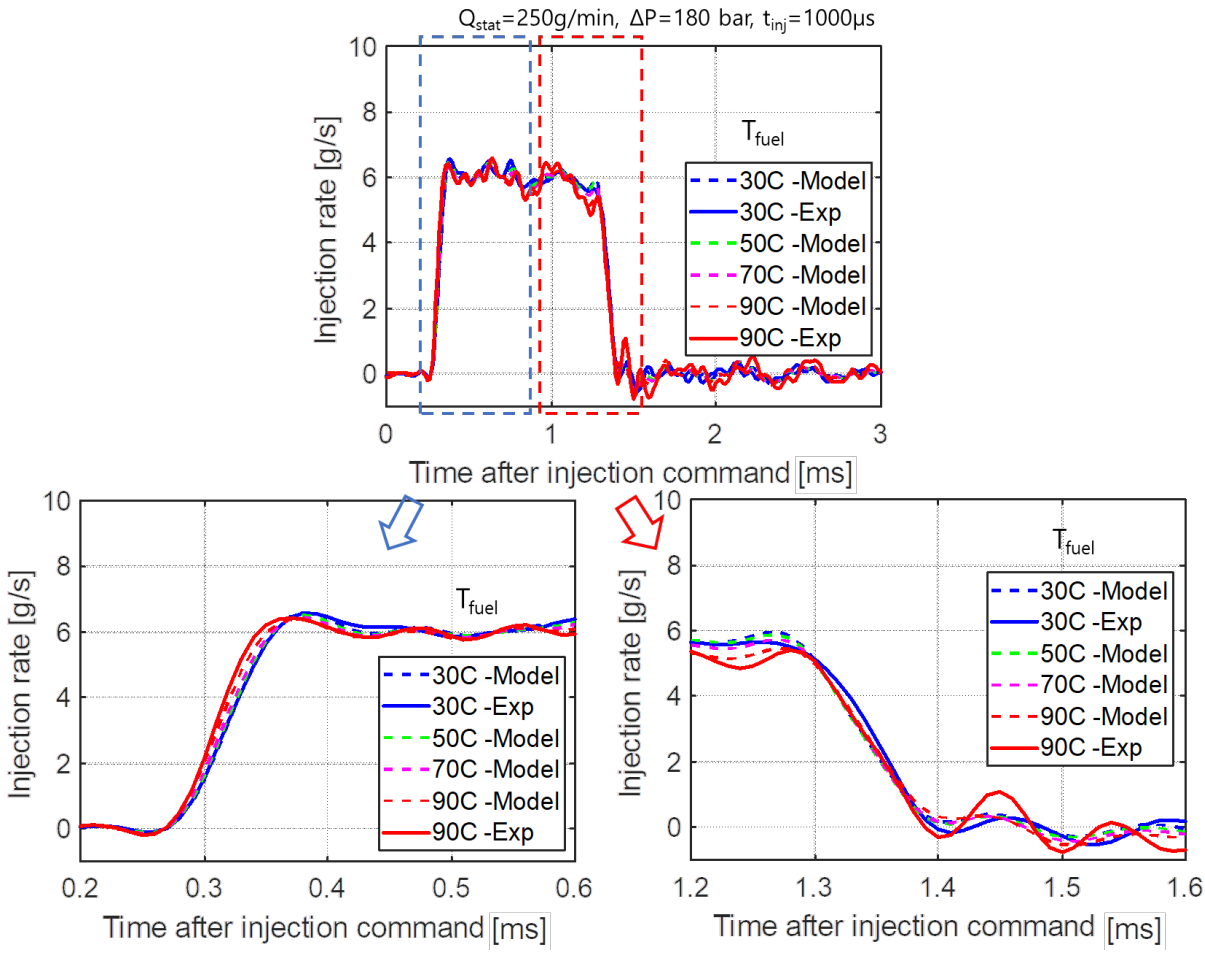


Figure 16. Modeled ROIs for different pressure difference under longer coil energizing time conditions.

https://doi.org/10.1016/j.fuel.2021.122569

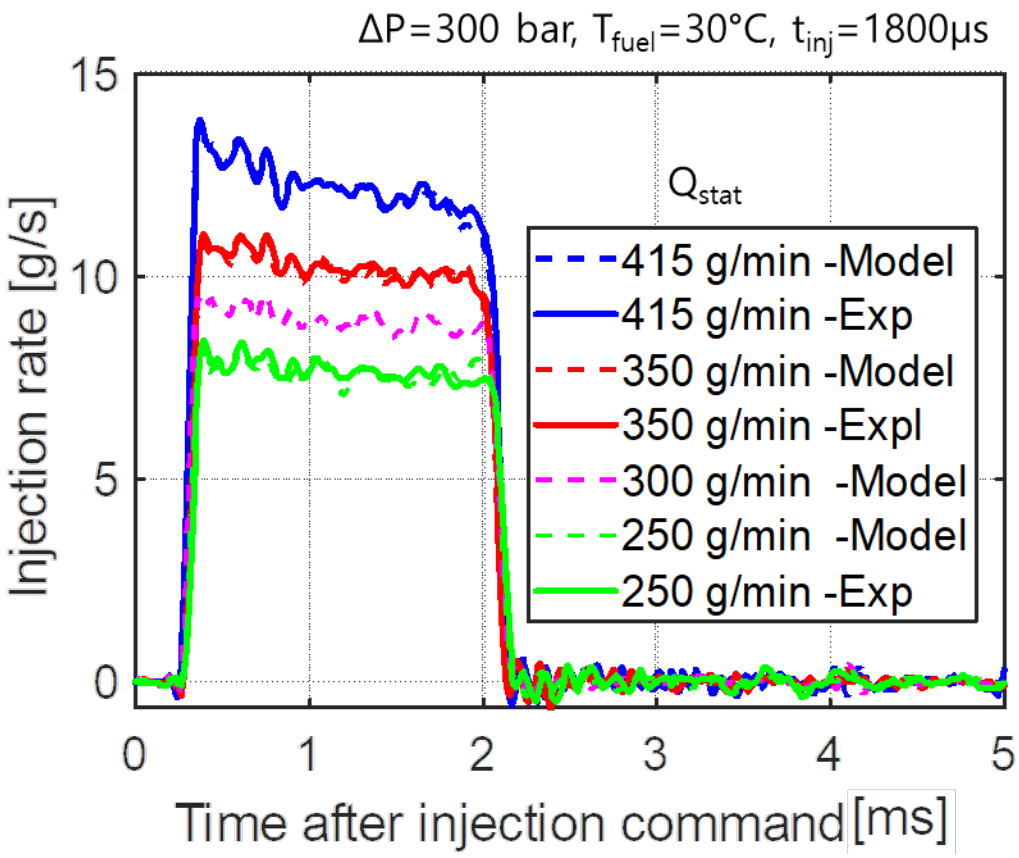


Figure 17. Modeled ROIs for different pressure difference under longer coil energizing time conditions.

https://doi.org/10.1016/j.fuel.2021.122569

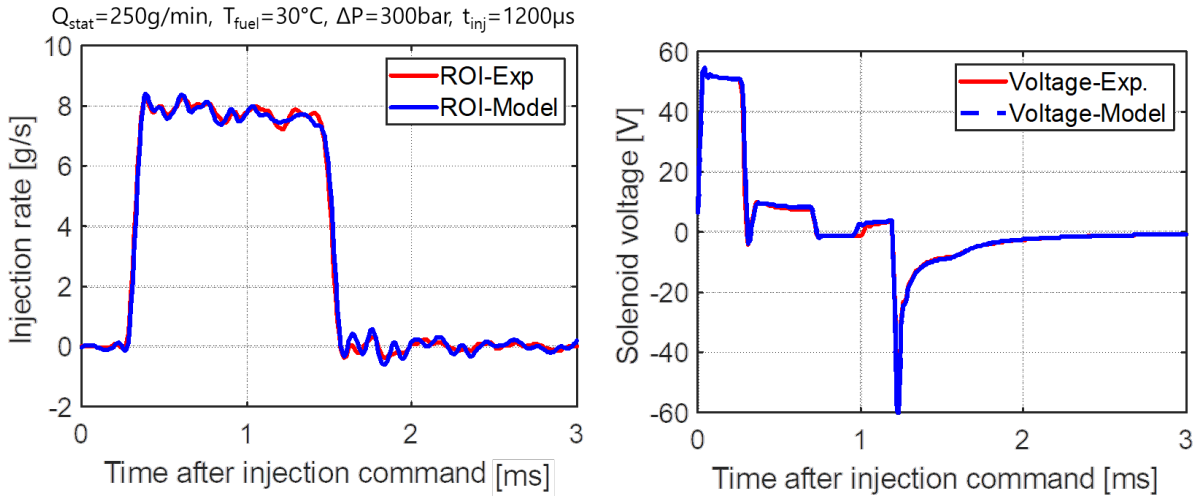


(a) Comparison of the measured solenoid voltage signal and the virtual signal generated by the regression model

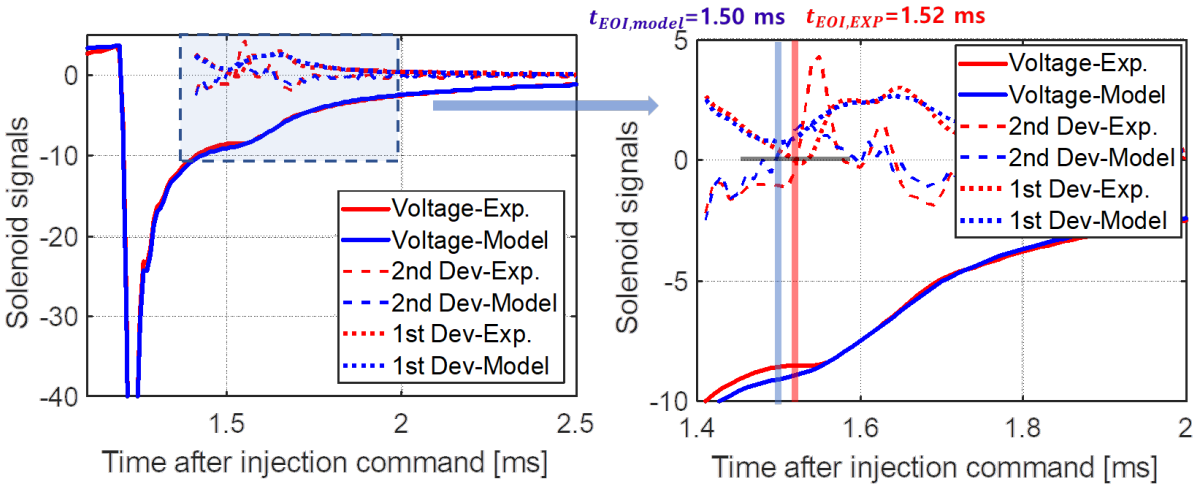


(b) Result of inflection point detection for modeled and measured solenoid voltage signals

Figure 18. Validation of modeled solenoid voltage signal

https://doi.org/10.1016/j.fuel.2021.122569

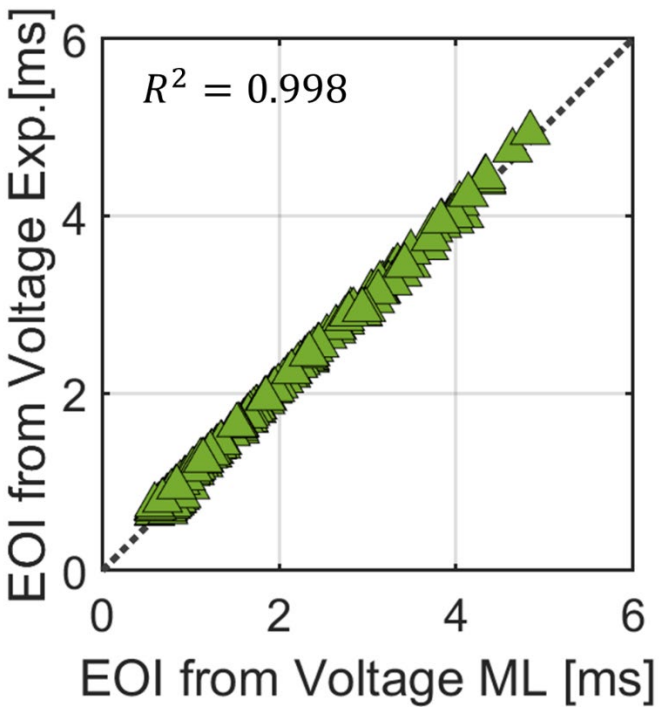


Figure 19. Correlation between end of injection timings from modeled and measured voltage signals